CHAPTER IV
ORGANO-MODIFIED BENTONITE CONTENTS INFLUENCED PROPERTIES OF PP/ORGANOMODIFIED BENTONITE NANOCOMPOSITE PACKAGING FILMS

4.1 Abstract

Na-bentonite was treated with quaternary alkyl ammonium cation, DOEM by ion exchange reaction. The d-spacing of organo-modified bentonite increases after treated with DOEM surfactant and the IR absorption of C=O bond and $-CH_2$ of surfactant occurred at 1740 and 2930 cm^{-1}.The ethylene gas adsorption capacity of Na-bentonite and organo-modified bentonite was determined by GC. The organo-modified bentonite was compounded with polypropylene by using Surlyn® ionomer as a compatibilizer. The polypropylene/organo-modified bentonite active packaging films were fabricated by using blow film extrusion method. The contents of organo-modified bentonite were varied as 1, 3, 5 and 7% in order to study the effect on the nanocomposites active packaging films. Dispersion of the organo-modified bentonites in the packaging film was observed by SEM. The ethylene gas permeability, thermal and mechanical properties of the nanocomposite active packaging films was investigated. The ethylene gas permeability of the nanocomposite films decreased when compared with polypropylene film. The degradation temperature of the nanocomposites packaging film was improved. Increased organo-modified bentonite loading enhanced the elastic modulus but decreased other tensile properties.

4.2 Introduction

One of the most common problems of post harvest fruits and vegetables is the limitation of their fresh and shelf-life. The new food-packaging systems have been developed as a response to trends in consumer preferences towards mildly preserved, fresh, tasty and convenient food products with a prolonged shelf-life. Traditional systems are reaching their limits with regard to further extension of shelf-life of packaged food. To provide this shelf-life extension, and to improve the quality, safety and integrity of the packaged food, innovative active and intelligent packaging concepts are developed. Active packaging changes the condition of the pack-aged food to extend shelf-life or improve food safety or sensory properties, while maintaining the quality of packaged food. Examples of active packaging systems are oxygen scavengers, ethylene absorbers, moisture regulators, taint removal systems, ethanol and carbon dioxide emitters, and antimicrobial releasing systems. Intelligent packaging systems monitor the condition of packaged food to give information about the quality of the packaged food during transport and storage. Typical examples of intelligent packaging include indicators of gas leaks, time-temperature history and microbial spoilage [1].

The main problem of a prolonged shelf-life of fresh fruits and vegetables is ethylene gas. Ethylene (C_2H_4) acts as a plant hormone that has different physiological effects on fresh fruit and vegetables. It accelerates respiration, leading to maturity and senescence, and also softening and ripening of many kinds of fruit. Furthermore, ethylene accumulation can cause yellowing of green vegetables and may be responsible for a number of specific postharvest disorders in fresh fruits and vegetables. To prolong shelf-life and maintain an acceptable visual and organoleptic quality, accumulation of ethylene in the packaging should be avoided. Ethylene can also be removed by using a number of chemical processes [2].

According to the structure of organo-modified bentonite which has high surface area, it can adsorb gas such as oxygen and ethylene gas [3]. When ethylene scavenger based on organo-modified bentonite blend with polypropylene, it can be applied as packaging film to improve the shelf-life of the fresh products.

All above ideas lead to the purpose of this work, the preparation of the ethylene scavenger film based on PP/organo-modified clay. The effect of clay mineral contents on the mechanical properties and thermal properties are also studied. X-ray Diffractometer (XRD), Fourier Trans-form Infrared Spectroscopy (FTIR), and Thermogravimetric Analysis (TGA) are used to characterize ethylene scavenger film. The ethylene gas permeability and the capable to use as ethylene scavenger film are also investigated.

4.3 Experimental

A. Materials

Na-bentonite (Mac-Gel® GRADE SAC) was supplied by Thai Nippon Co., Ltd. Thailand and DOEM surfactant (Stepantex VB 85) was supplied by Union Carbind Co., Ltd. Thailand. Ethanol 99.8% v/v was commercially purchased from Carlo Erba. PP under commercial name of Polene (1126 NK), MFI =11 was commercially purchased from IRPC Public Co., Ltd. Thailand. The compatibilizer, Surlyn® ionomer (PC 350) was supplied by DuPont (Thailand) Co. Ltd.

B. Preparation of organo-modified bentonite

In container, 350 g of Na-bentonite was swollen in 10 L of water for 24 hr, and in another container DOEM as an alkyl ammonium ion (1.5CEC) was dissolved in 1600 ml of water/ethanol (1/1, v/v) solution. Then, the solution was heated at 80 °C until it became transparent. Then solutions of two containers were vigorously mixed for 2 hr at 80 °C 1000 rpm and homogenized at 600 rpm for 30 min. The organo-modified bentonite was filtered and washed with hot water several times. It was dried in a vacuum oven at 100 °C overnight and ground into 325 mesh under [4, 5].

The surface area of clay mineral was observed by using Thermo Finnigan, Soptomatic 1990 from Quanta Chrom Company.

The change of interlayer distance was measure by wide angle X-ray diffraction (WAXD) using a Rigaku Model Dmax 2002 diffractometer with Ni-filtered Cu

K_α radiation operated at 40 kV and 30 mA. The scanning range was 2θ = 1.2-2.0° with scan speed 2 degree/min and scan step 0.01 degree.

Infrared spectra (IR) of clays were obtained by using a Nicolet Nexus 670 FT-IR spectrometer over a wave number range of 4,000-400 cm^{-1} with 32 scans at a resolution of 2 cm^{-1}.

The content of the organic component was determined by TGA using a Perkin-Elmer Pyris Diamond TG/DTA instrument. The heating process was carried out from 30-800°C at a rate of 10°C/min in the nitrogen atmosphere of 200 ml/min.

The reduction of ethylene gas by the clay mineral was determined by gas chromatography, Algilent Technologies 6890 Network GC system, using HP-PLOT Q column: 30 m x 0.32 mm ID and 20 μm film thicknesses. A detector was FID type using He as the carrier gas. The initial temperature was 150 °C and holding time was 10 minutes. The 500 ml glass chamber was pursed by nitrogen gas and contain 15 g of organo-modified bentonite then closed the chamber with rubber stopper with the rubber septum in the middle of the stopper as shows in Figure 4.1. 500 ppm of ethylene gas was loaded into the chamber and sampling 5 ml of gas every 1 hr injected into GC [6].

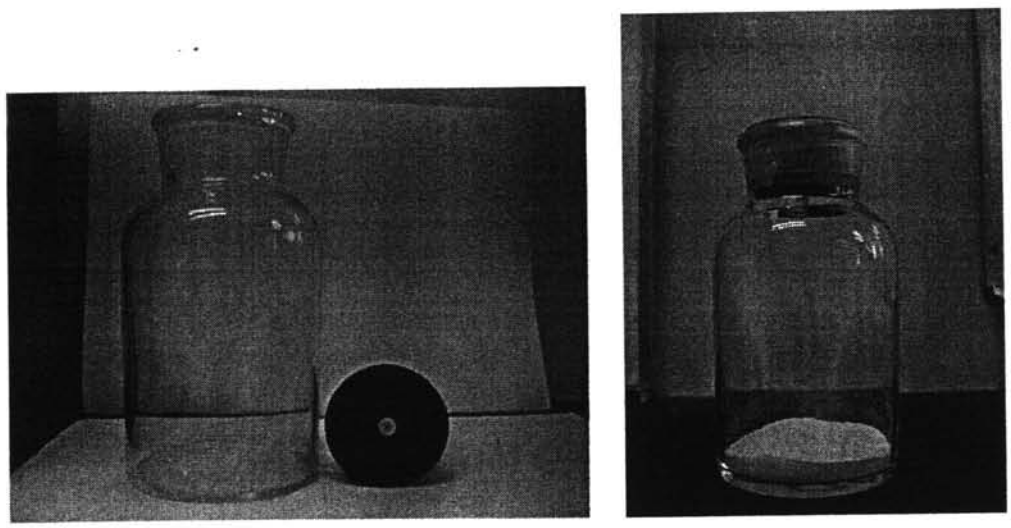

Figure 4.1 Chamber preparation for ethylene gas reduction testing.

C. Preparation of PP/organo-modified bentonite nanocomposite films

Polypropylene was blended with 6%wt of Surlyn® ionomer by using a Model T-20 co-rotating twin-screw extruder (Collin) with L/D=30 and D=25 mm. The operating temperatures of extruder were maintained at 80, 170, 180, 190, 200, and 210°C from hopper to die, respectively. The screw speed was 50 rpm. The obtained pellets were dried under vacuum at 80^0C. Polypropylene with compatibilizer was dry-mixed with 1, 3, 5, and 7% wt of organo-modified bentonite by shaking them in an internal-mixer for 10 min. Then , they were melt mixing by twin screw extruder, a Model T-20 co-rotating twin-screw extruder (Collin) with L/D=30 and D=25 mm. The operating temperatures of extruder were maintained at 80, 170, 180, 190, 200, and 210°C from hopper to die, respectively. The screw speed was 50 rpm. After drying , the composite pellets were fabricated into the packaging film by tubular blown film extrusion. The screw speed was 50 rpm, screw diameter was 45 mm, L/D was 26 and the processing temperature were 210 °C from hopper to die.

The contents of the inorganic clay of the nanocomposites were measured by burning the sample in a Perkin-Elmer Pyris Diamond TG/DTA Analyzer. The crystallization and melting behaviors of the PP/organo-modified bentonite nanocomposites were measured with a Perkin-Elmer DSC 7 analyzer. During the crystallization experiment, the specimens were first melted at 250°C, and then cooled to room temperature at 10°C/min rate. The specimens were subsequently heated at 10°C/min for the corresponding melting behavior investigations.

The crystal structures of PP/organo-modified bentonite nanocomposites were also analyzed by Wide angle X-ray diffraction (WAXD) using a Rigaku Model Dmax 2002 performed in the 2θ of 2-50 degrees with the scan speed 2θ/min.

The dispersion of organo-modified bentonite in the nanocomposites film was observed by SEM (JEOL/JEM 5800 LV) and TEM (Phillip, TECH-NAI). Ultrathin sectioning was performed with a Reichert FCS microtome equipped with a diamond knife.

The aluminium contents in the nanocomposite films were determined by EDX mode of SEM and AAS. The nanocomposite films were heat at 450 °C for 1 hr.

The residual was digested by hydrofluoric acid (HF) to prepare the sample solution then analyzed by using Varian, StectrAA 300.

Tensile tests were performed at room temperature according to ASTM D882 using a Lloyd Universal Testing Machine. The specimen dimension is 10x150 mm. Yield strength and strain at break were measured using an extensometer at a cross-head speed of 50 mm/min, load cell 500 N. The data reported from seven specimens were averaged to determine mechanical properties.

Ethylene gas permeability was measured according to ASTM D1434 by using GDP/E Brugger Munchen. Determine the slope of the graph, N by dividing the time (s) by the scale division (mm). The gas permeability rate, G in units of $cm^3/ (m^2.day.bar)$ is calculated from

$$G = \frac{77.76x10^{10}xV}{78.5Kx29N}$$

where V = volume of the evacuation chamber = 0.4370 cm^3

K = absolute temperature (degrees Kelvin) = 300 K

Ethylene gas permeability, P in units of $ml(STP)/m^2.d.atm$ is calculated from

$$P = G \times T \times 5.164 \times 7.725$$

where T = thickness of polymer films (mm) = 0.03 mm

4.4 Results and Discussion

A. Characterizations of the organo-modified bentonite

Fig.4.2 displays the X-ray diffraction patterns of both modified and unmodified bentonite clay. The d_{001} peak of pristine Na-bentonite clay at $2\theta = 7.19^{o}$ corresponds to basal spacing of 1.23 nm. It can be observed the d_{001} peak shift to the lower angle, corresponding to an increase on the basal spacing of the clay, 3.75 nm and 7.11 nm, by exchange of interlayer with alkylammonium ions. However, this modified bentonite shows broad peaks at the lower angles due to the inhomogeneous distribution of the surfactant between the layers of the clay, presenting a broader range of interlayer distances depending on the extent of ion exchange [7].

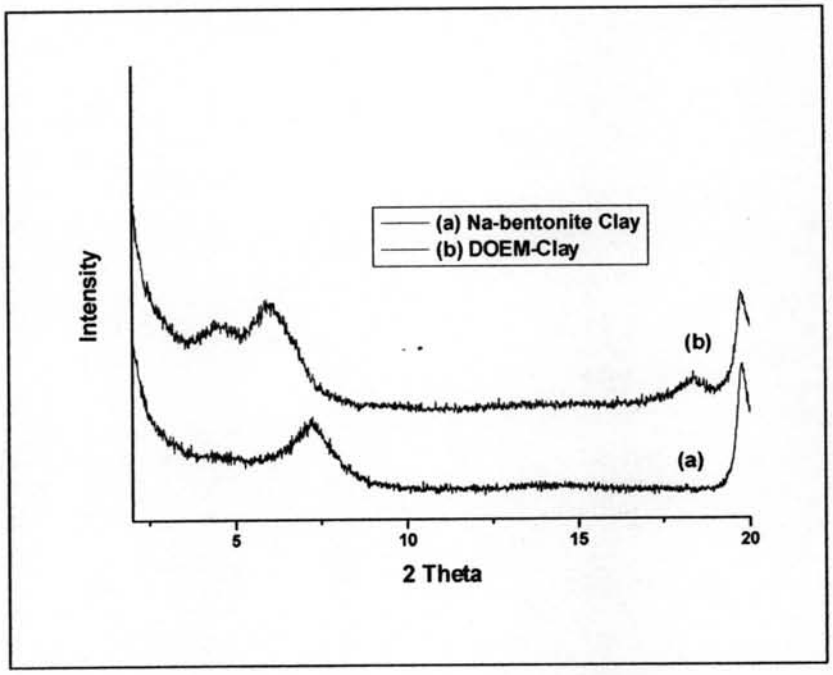

Figure 4.2 The WAXD patterns of organo-modified bentonite: (a) Na-bentonite clay and (b) DOEM-Clay.

The presence of the organo-surfactant was confirmed by FT-IR. Figure 4.3 shows the FT-IR spectra of Na-BTN and organo-modified bentonite. A pair of strong bands near 2850 and 2930 cm^{-1} at each spectrum can be assigned to the symmetric and asymmetric stretching vibration of methylene group (υCH_2) of the guest molecules. Na-BTN organo-modified with DOEM, including ether group, has an absorption band at 1740 cm^{-1} due to the stretching vibration of the carbonyl group (>C=O)[8].

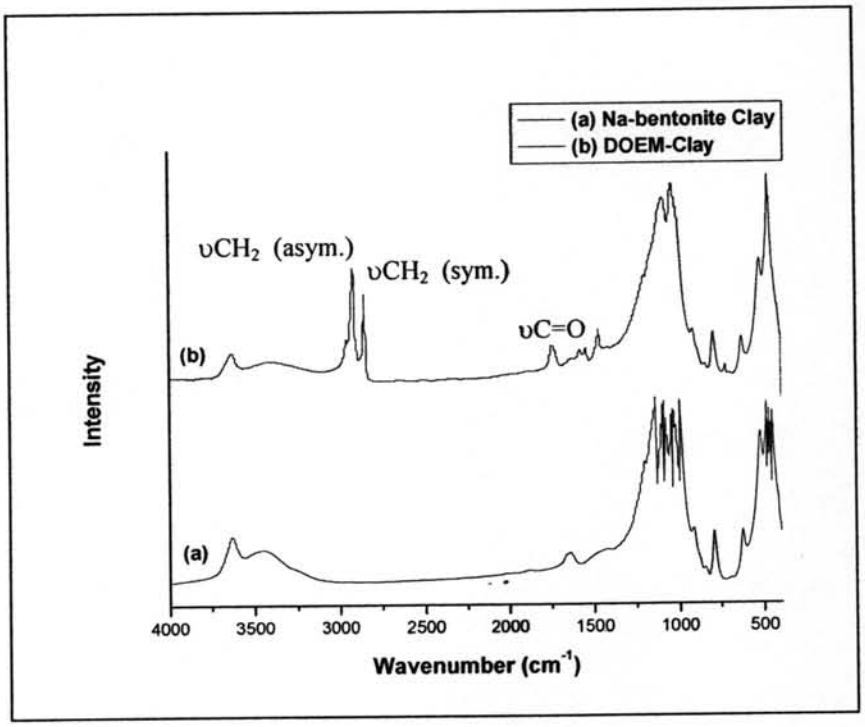

Figure 4.3 Infrared spectra of organo-modified bentonite: (a) Na-bentonite, (b) DOEM-Clay.

The thermal behavior of Na-bentonite and organo-modified bentonite were represented in Table 4.1. The content of the organic component was determined from the weight loss during TGA. For Na-bentonite, there was two main mass loss steps, the first mass loss step due to the dehydration was observed over temperature range of 52.0-66.5°C with 3%mass loss. The other step was attributed to the structural OH unit of clay from 569.9 to 681.9°C, about 3.4 %mass loss. On the organo-modified

bentonite the weight-loss of water desorption was around 1% and very large amount of weight-loss was shown at the temperature range of 250–450^{0}C, which was related to the thermal decomposition of the organo-surfactant [9].

Table 4.1 Thermal behavior of clay mineral

Sample	Mass Loss H_2O (wt %)	Mass Surfactant		Char Residual (wt %)	Desurfactant		
		wt%	mole		T_d (°C)	T_i (°C)	T_f (°C)
Na-bentonite	0.7	-	-	96.0	-	-	-
DOEM-clay	0.9	28.2	0.04	58.5	351.4	246.4	364.8

B. Ethylene gas reduction of organo-modified bentonite

The surface area of Na-bentonite and organo-modified bentonite are 28.93 and 3.60 m^2/g respectively. The surface area of bentonite decreases due to the interaction of the surfactant on its surface. The reduction of surface area cause to reduce the adsorption sites on the clay surface and the ethylene gas reduction of organo-modified bentonite should be higher different from Na-bentonite but from the results Na-bentonite reduces ethylene gas 2.4% faster than DOEM-Clay. This suggests that, although DOEM-bentonite has much lower surface area than Na-bentonite, DOEM surfactant provides higher acidity to clay surface thus it prefers to react with double bond of ethylene gas [10, 11].

The ethylene gas reduction of Na-bentonite and organo-modified bentonite are shown in Fig. 4.4. The initial concentration of ethylene gas is 33.33 ppm/g after 9 hours the concentration of ethylene gas is reduced with the time. These results showed that Na-bentonite clay and organo-modified bentonite can reduce ethylene gas by adsorb ethylene gas on their surface.

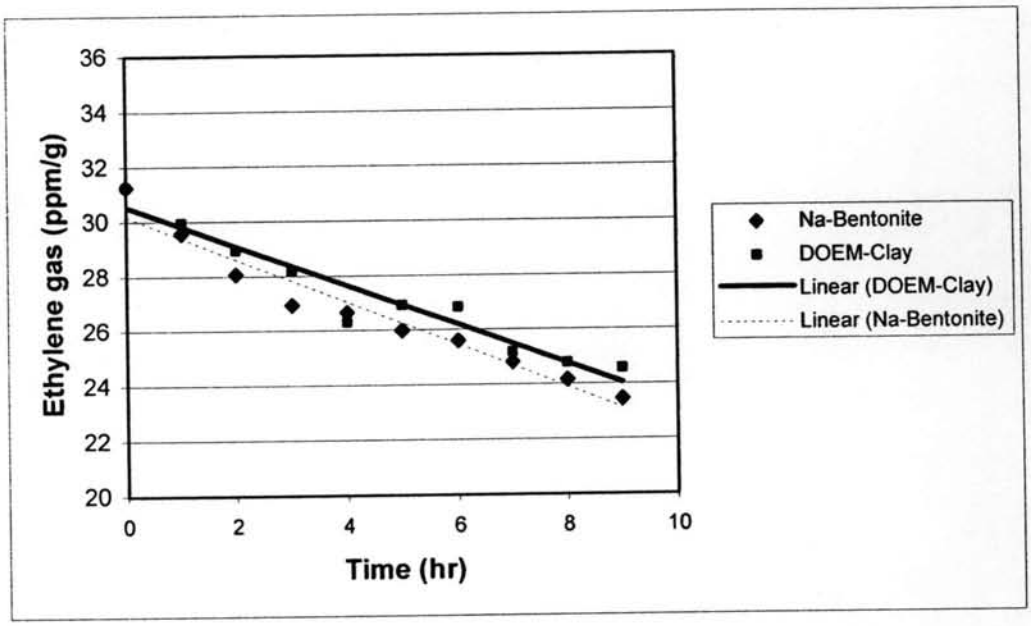

Figure 4.4 Ethylene gas reduction of Na-bentonite and DOEM-Clay.

C. Thermal behavior of PP/organobentontie nanocomposite films

The melting and crystallization behavior, as measured by DSC, of PP and PP/organo-modified bentonite nanocomposite films are shown in Figure 4.5 and Table 4.2. DSC scanning was carried out in the temperature rang between 30-250 °C correspondind to the melting point of PP (160-170 °C). Compared with pure PP, the PP/organo-modified bentonite nanocoposite films have lower % crystallinity, melting temperature and crystallization temperature. The reason should be attributed to the disturbance of crystalline formation induced by the organo-modified bentonite in the system during cooling process [12].

Table 4.2 Melting and crystallization behavior of PP and PP/organo-modified bentonite nanocomposite films

Films	T_m (°C)		T_c (°C)		ΔH_m (J/g)	Crystallinity (%)
	Onset	Peak	Onset	Peak		
PP	157.68	163.03	121.28	116.13	88.85	42.51
PP/Surlyn	155.71	160.37	116.56	111.30	86.44	38.88
PP/Surlyn/1%Clay[1]	156.46	160.70	116.37	112.80	85.69	38.13
PP/Surlyn/3%Clay	157.61	162.37	119.38	114.63	81.35	35.42
PP/Surlyn/5%Clay	156.16	161.37	117.66	112.97	81.90	34.88
PP/Surlyn/7%Clay	156.25	160.53	116.76	112.80	80.14	33.36

PP 100% Crystallinity, $\Delta H_m = 209$ J/g

[1] x % Clay = x% wt of DOEM-Clay in nanocomposites

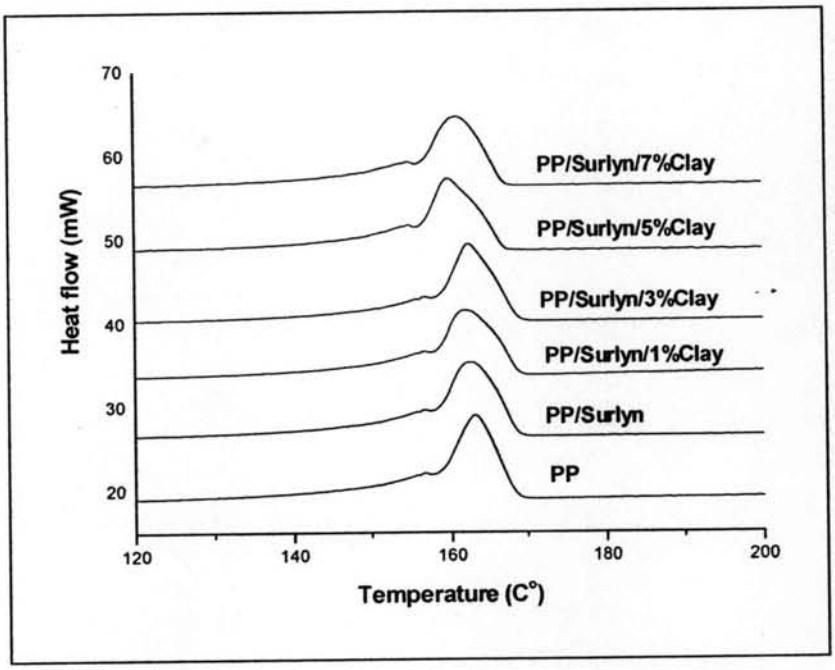

(a)

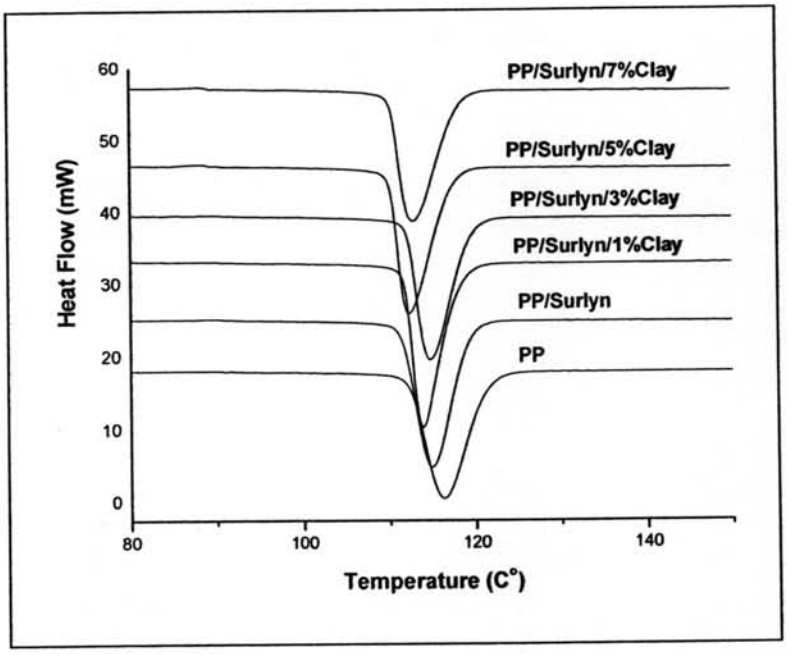

(b)

Figure 4.5 DSC thermograms of PP/organo-modified bentonite nanocomposites film (A) Melting Temperature, and (B) Crystallization Temperature.

Summary of TGA experimental results for the nanocomposite films is shown in Table 4.3 and Figure 4.6 and 4.7. The incorporation of organo-modified bentonite into PP improved the degradation temperature. The presence of metal oxides in organo-modified bentonite such as silica, aluminium and magnesium was attributed to this improvement [13].

Table 4.3 Thermal behavior of PP and PP/organo-modified bentonite nanocomposite films

Sample	TGA			
	Residual (wt%)	T_d (°C)	T_i (°C)	T_f (°C)
PP	-	454.50	432.80	487.40
PP/Surlyn	-	454.70	435.10	487.80
PP/Surlyn/1%Clay	0.50	457.70	437.30	489.50
PP/Surlyn/3%Clay	1.20	459.90	439.00	487.90
PP/Surlyn/5%Clay	3.33	454.40	432.70	468.10
PP/Surlyn/7%Clay	5.00	459.00	436.00	469.00

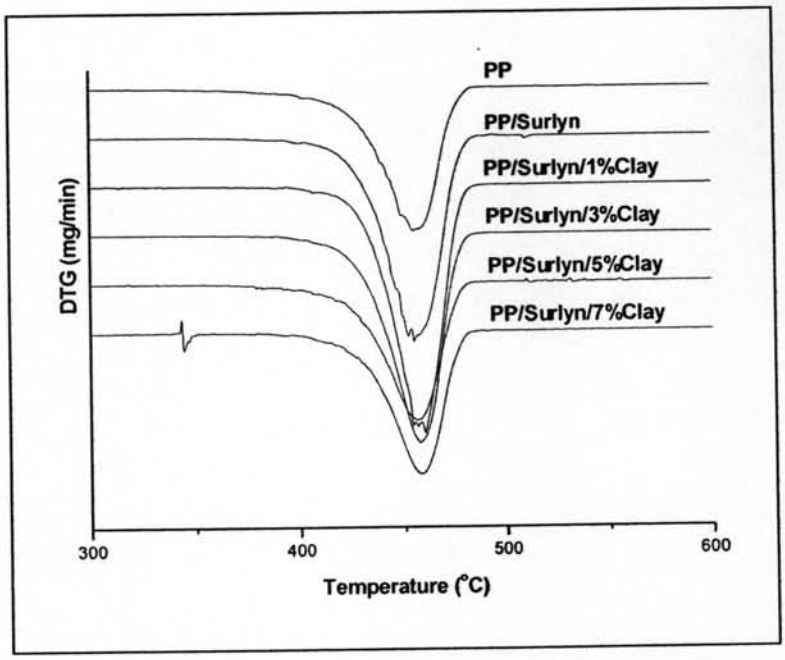

Figure 4.6 DTA curves of PP/organo-modified bentonite nanocomposite films.

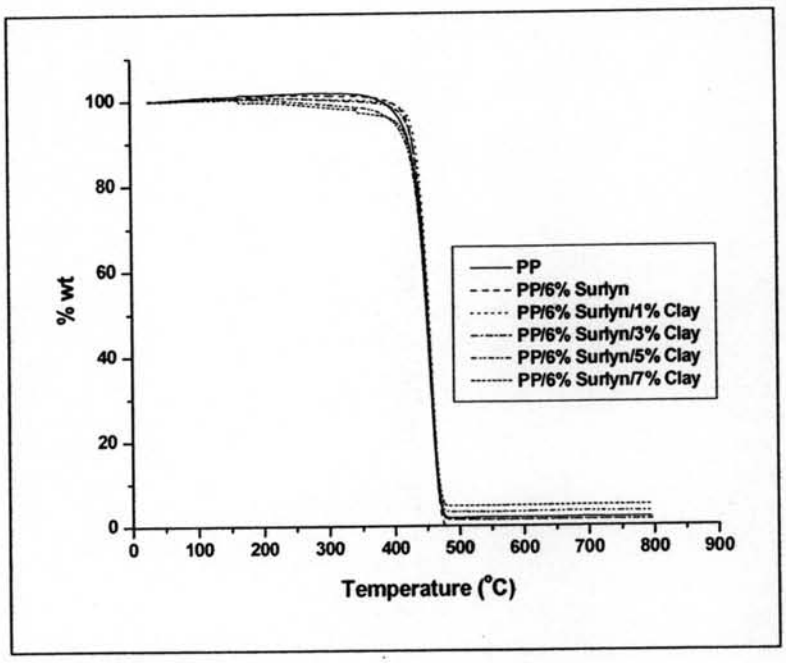

Figure 4.7 TG curves of PP/organo-modified bentonite nanocomposite films.

D. Crystallization behavior of PP/organo-modified bentonite nanocomposite films

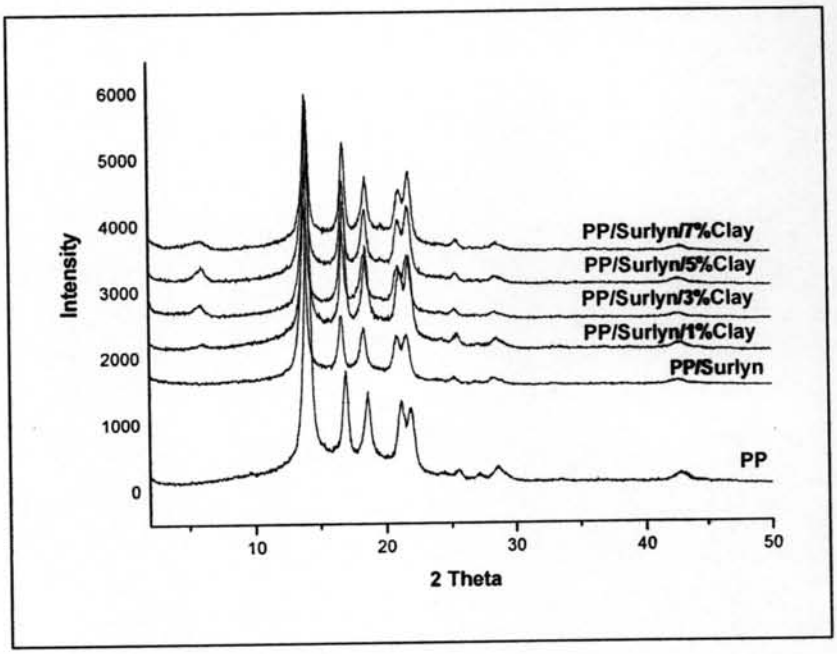

(a)

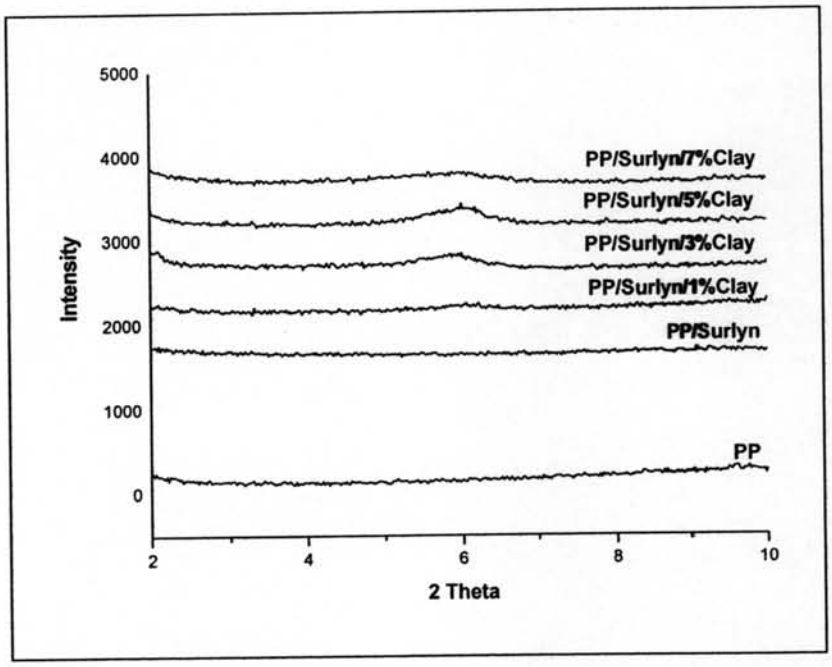

(b)

Figure 4.8 The XRD patterns of PP and PP/organo-modified bentonite nanocomposite film films (a) 2θ = 2-50° and (b) 2θ = 2-10°.

The structure of the nanocomposites was examined by XRD. The characteristic PP crystal peaks were analyzed with in the 2θ range of 2-50°, as shown in Fig. 4.8 (a). Pristine PP shows five prominent which correspond to monoclinic α crystalline phase: α_1, α_2, α_3 and α_4 belong to the (110), (040), (130) and (111, 041) reflection corresponding to 2θ = 14.04, 16.86, 18.50. 21.08 and 21.72, respectively. The PP/organomodified clay nanocomposites show the same corresponding peak with pristine PP that mean the organo-modified bentonite does not affect on the structure of PP crystal [14].

From Fig. 4.8 (b) the peaks correspond to the (001) reflections of the clay. It can not be observed in the XRD patterns of nanocomposite with 1% organo-modified bentonite suggesting that the silicate clay layers have a nearly exfoliated dispersion in the polymer matrix. When organo-modified bentonite contents in nanocomposite are increased the corresponding peak occurred at 2θ around 6° that means the intercalations of PP into the organo-modified bentonite layer are occurred [15].

E. Mechanical properties of PP/organo-modified bentonite nanocomposite films

Figure 4.9 shows that the Young's modulus of the nanocomposite films slightly increased with increasing organo-modified bentonite loading. This result effected from the high modulus and high aspect ratio of organo-modified bentonite. These effects increase the stress and reduce the strain of the nanocomposites films so that the Young's modulus of the nanocomposite films increases [16].

Figure 4.10 show the effect of organo-modified bentonite loading on tensile strength of PP films. The tensile strength is reduced as the percent of organo-modified bentonite increases. The incorporation of organo-modified bentonite into PP matrix reduced the ability of the composites to transfer applied stress. In addition, the agglomeration of the organo-modified bentonite can act as a stress concentration point and increase the chance of the composites to initiate cracks [16].

The effect of organo-modified bentonite on elongation at break is shown in Figure 4.11. Adding organobentnite into PP matrix decreases the elongation at break, due to the organobentonite obstructing the movement of PP along the applied force [16].

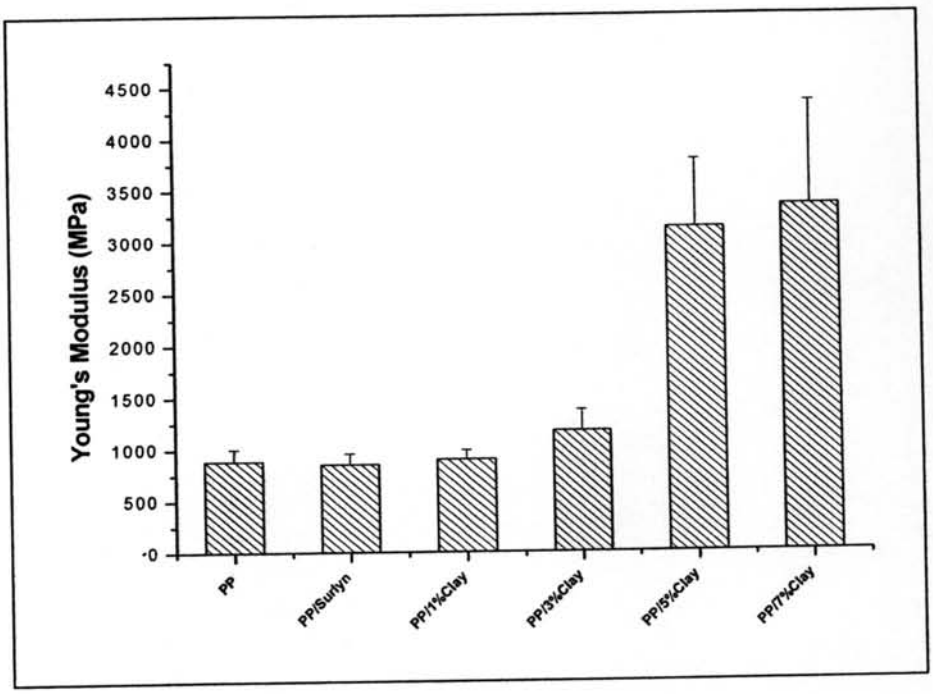

Figure 4.9 Young's modulus of PP and PP/organo-modified bentonite nanocomposite films with various organo-modified bentonite loading.

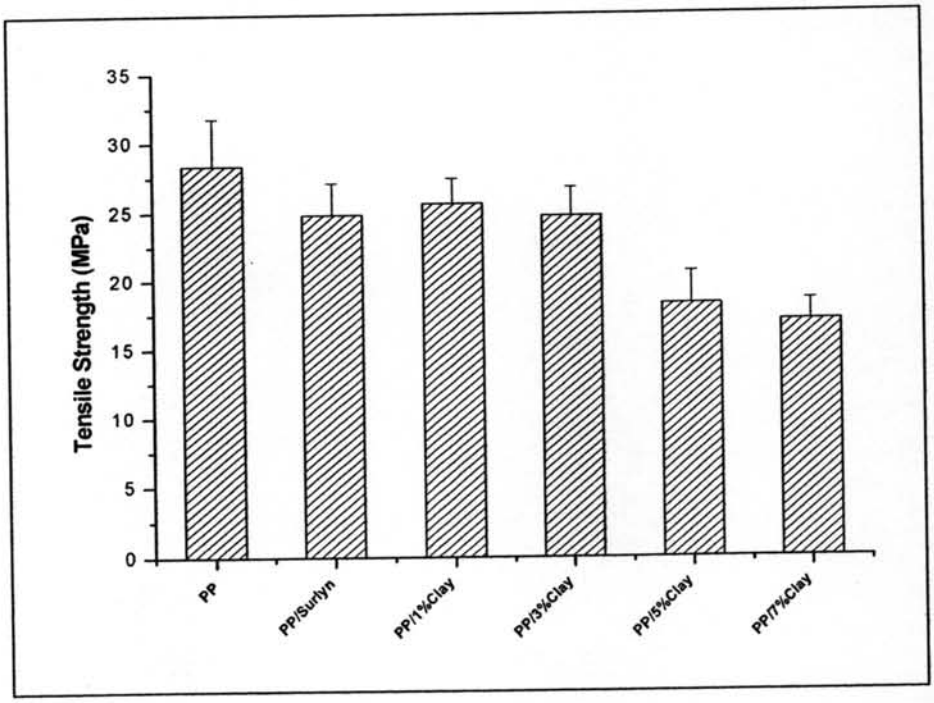

Figure 4.10 Tensile strength of PP and PP/organo-modified bentonite nanocomposite films with various organo-modified bentonite loading.

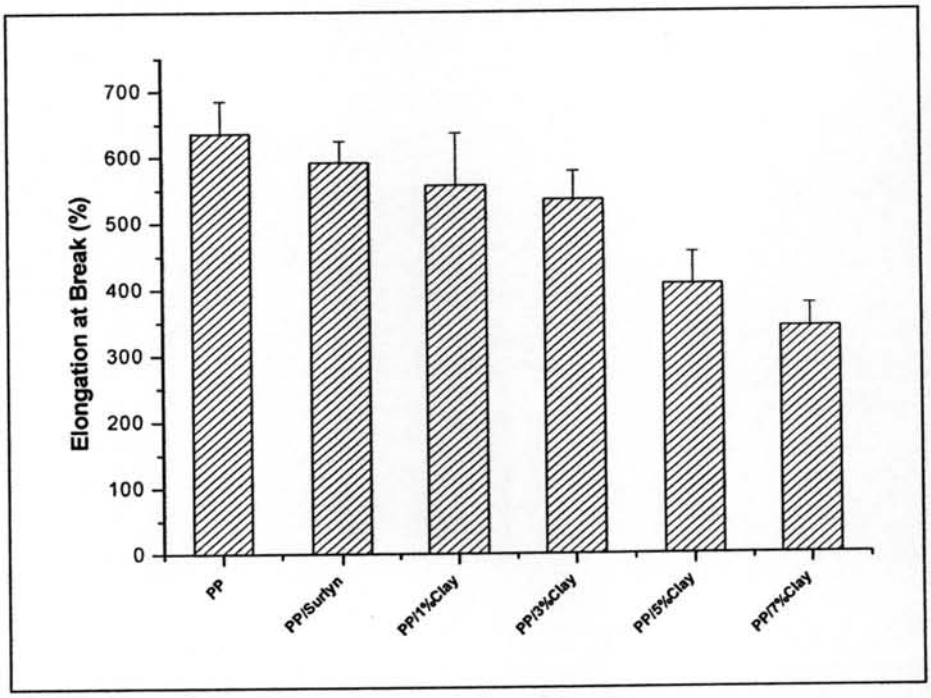

Figure 4.11 Elongation at break (%) of PP and PP/organo-modified bentonite nanocomposite films with various organo-modified bentonite loading.

F. Dispersion of organo-modified bentonite in nanocomposite films

Figure. 4.12 shows the dispersion of organo-modified bentonite and the dispersion of Si and Al by EDX mode in nanocomposites films. When the clay content increases, the accumulation of the organo-modified bentonite occurred on the films as the small nodules in the nanocomposite films. These affect the reduction of the tensile properties in the packaging films [17].

The amount of element which obtained by EDX mode of SEM and AAS show in Table 4.4 and Table 4.5 indicated that when the clay content increases the amount of Al and Si also increase.

Table 4.4 Percent element on surface of PP/organo-modified bentonite nanocomposite films by EDX

Sample	% Element			
	C	O	Al	Si
PP/Surlyn/1%Clay	94.56	4.91	0.03	0.50
PP/Surlyn/3%Clay	93.53	5.63	0.11	0.73
PP/Surlyn/5%Clay	92.88	6.07	0.11	0.94
PP/Surlyn/7%Clay	93.50	5.13	0.21	1.16

Table 4.4 Percent Al in PP/organo-modified bentonite nanocomposite films by AAS

Sample	Al (ppm)	Al (%wt)
PP/Surlyn/1%Clay	13.1	6.06
PP/Surlyn/3%Clay	14.5	6.73
PP/Surlyn/5%Clay	22.0	10.36
PP/Surlyn/7%Clay	22.6	10.46

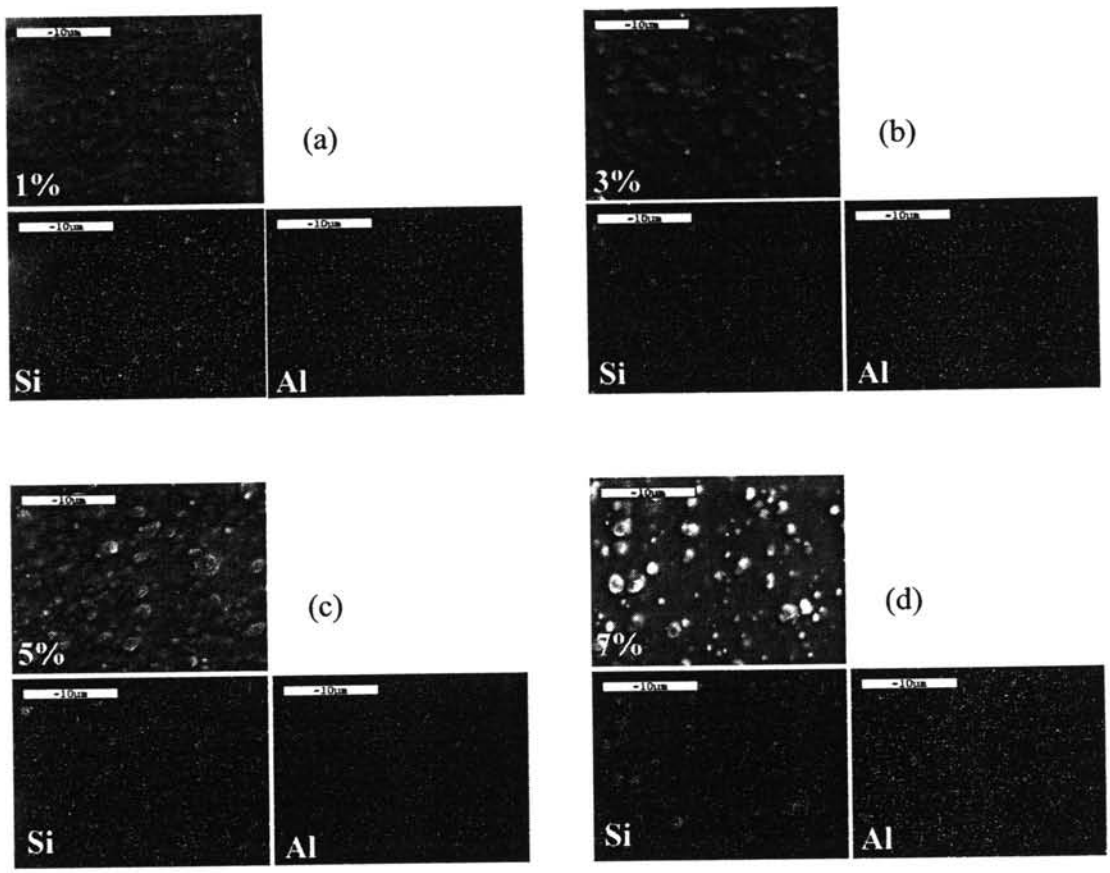

Figure 4.12 SEM images and Al, Si mapping of organo-modified bentonite in nanocomposite films (a) 1% Clay (b) 3% Clay (c) 5% Clay (d) 7% Clay .

TEM images in the Figure. 4.13 show that intercalation occurred in the PP/organo-modified bentonite active packaging films and it can confirm by XRD patterns in Fig. 4.8. They were not completely exfoliated because the shear force is not high enough to overcome the residual attraction between all clay platelets [18].

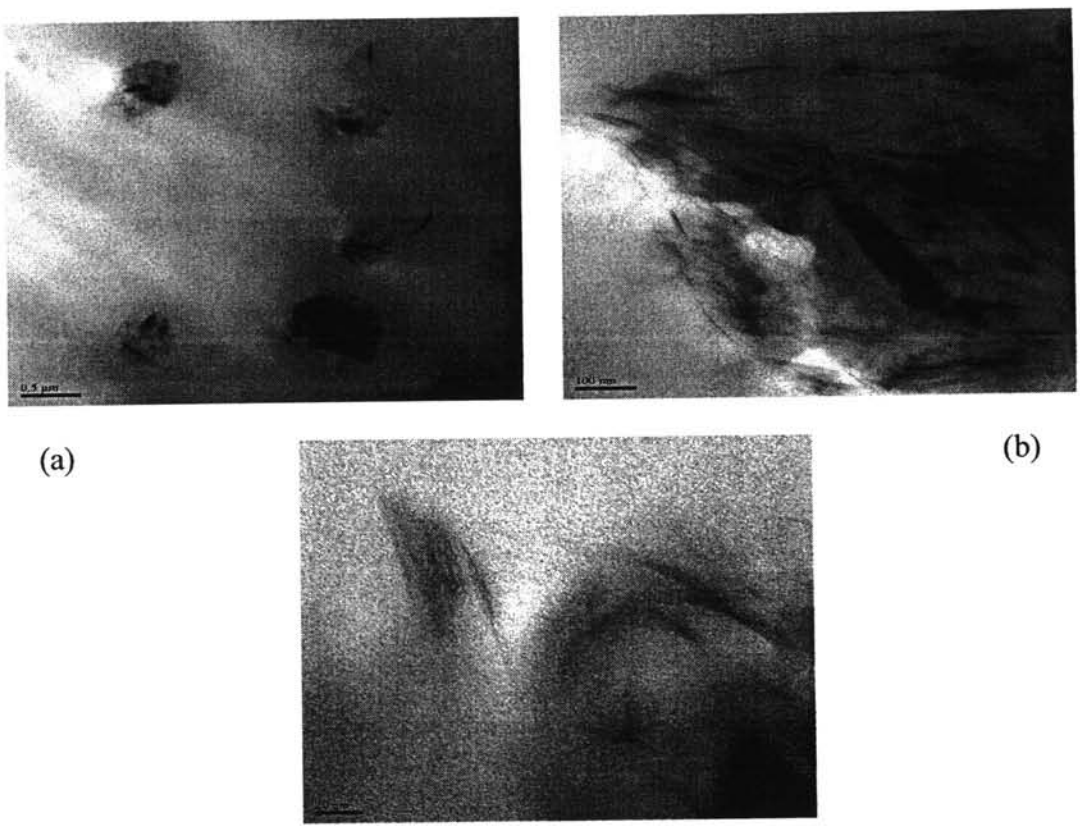

(a) (b)

(c)

Figure 4.13 High-resolution TEM images of PP/organo-modified bentonite nano-composite film.

G. Ethylene gas permeability of PP/organo-modified bentonite nanocomposite films

Ethylene permeability of the organo-modified bentonite-filled PP films are compared with pure PP film and shown in Figure. 4.14. The reduction of ethylene gas permeability due to barrier property from the presence of organo-modified bentonite in PP film and the adsorption of the ethylene molecule on the organo-modified bentonite surface. Although, crystallinity decreases by addition of organo-modified bentonite as shows in the small Figure. This shows the effect of flake-like filler in barrier improvement given that crystalline parts are less permeable than amorphous domains. Adding clay filler, improves barrier properties due to the combination of two phenomena: 1) the decrease in area available for diffusion, a result of impermeable flakes replacing permeable polymer; 2) the increase in the distance a solute must travel to cross the film as it follow a tortuous path around the impermeable flakes [19,20].

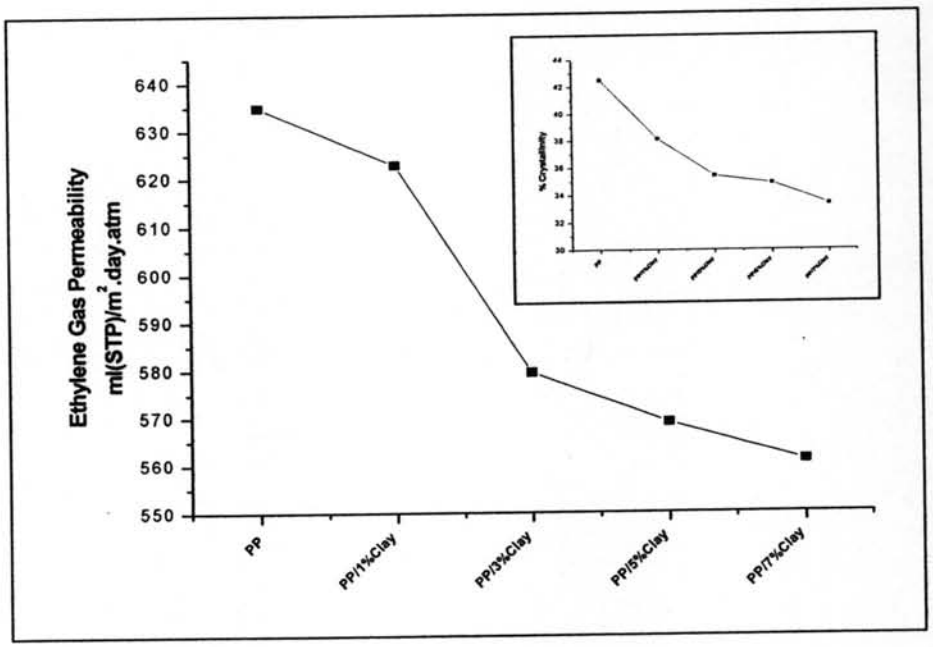

Figure 4.14 Ethylene gas permeability of PP/organo-modified bentonite nanocomposites films.

4.5 Conclusions

Both of Na-bentonite and organo-modified bentonite which is treated with DOEM surfactant show the ability to adsorb ethylene gas on the clay surface by van der Waals force and the interaction of higher acidity DOEM-clay with double dond of ethylene gas. When the organo-modified bentonite is mixed with PP to fabricate the active packaging film by vary the content of organo-modified bentonite the intercalation is occurred in the nanocomposite films. The degradation temperatures increase by increasing the clay contents but melting temperature and crystallization temperature decreased. In addition, the organo-modified bentonite can improve the Young's modulus of the films when increasing the organo-modified bentonite content but tensile strength and elongation at break decrease by increasing the organo-modified bentonite content. When the organo-modified bentonite content in the packaging film increase, the agglomeration occurs as shown in the SEM images. These agglomerations drop the tensile properties of the films. The ethylene gas permeability constant reduces when increasing the organo-modified bentonite content. These results indicated that PP/organo-modified bentonite nanocomposite films can be used as ethylene scavenger active packaging film to extend the self life of fresh fruits and vegetables.

4.6 Acknowledgements

This work is funded by the National Research Council of Thailand, Polymer Processing and Polymer Nanomaterial Research Units and Petroleum and Petrochemical Technology (PPT) Consortium. The authors would like to thank Thai Nippon Chemical Industry Co, Ltd., for providing the raw materials carried out this research and Tang Packaging Co., Ltd. for tubular blown film extrusion machine. Dr. Vivan Thammongkol, Petroleum authority of Thailand, BKK for providing ethylene gas.

4.7 References

1 R. Ahivenainen, and M. Smolander. "Novel Food Packaging Techniques". Cambridge England: Woodhead Publishing Limited, (2003), 1-50.

2 Y. Wang, A.J. Easteal and X. Dong. "Ethylene and oxygen permeability through polyethylene packaging films" *Packaging Technology and Science*, **11**(1998), 169-178.

3 A. Cheng, W. Huang. "Selective adsorption of hydrocarbon gases on clays and organic matter" *Organic Geochemistry,* **35**(2004), 413-423.

4 J.Y. Lee, H.K. Lee. "Characterization of organobentonite used for polymer nano-composites" *Material Chemistry and physics,* **85**(2004), 410-415.

5 R.K. Shah, D.R. Paul. "Organoclay degradation in melt processed polyethylene nanocomposites" *Polymer,* **47**(2006), 4075-4084.

6 G. Peiser, T. Suslow. "Factor affecting ethylene adsorption by zeolite" *Perish-ables Handling Quarterly,* **95**(1998), 17-19.

7 Y. Kim, J.L. White. "Formation of polymer nanocomposites with various or-ganoclays" *Applied Polymer Science,* **96**(2005), 1888-1896.

8 J. Choy, S. Kwak, Y. Han and B. Kim. "New organo-montmorillonite complexes with hydrophobic and hydrophilic functions" *Materials Letters*, **33**(1997), 143-147.

9 Y. Xi, Z. Ding and R.L. Frost. "Structure of organo-clays-an X-ray diffraction and thermogravimetric analysis study" *Colloid and Interface Science,* **227**(2004), 116-120.

10 K. Kosuge. "Layered polysilicate gas adsorption properties and dispersion of the particles" *Clay Science Society of Japan,* **33**(1994), 215-222.

11 F. Wypych. K.G. Satyanarayana. "Clay Surfaces: Fundamentals and Applica-tions" *Interface Science and Technology,* **1**(2004), 290-345.

12 S. Parija, S.K. Nayak, S.K. Verma, and S.S. Tripathy. "Studies on physico-mechanical Properties and thermal characteristics of polypropylene/layer silicate nanocomposites" *Polymer Composites,* **25**(2004), 646-652.

13 H. Qin, S. Zhang, C. Zhao, G. Hu, and M. Yang. "Flam retardant mechanism of polymer/clay nanocomposites based on polypropylene " *Polymer,* **46**(2005), 8386-8395.

14 F. Chiu, S.Lai, J. Chen, and P. Chu. "Combined effect of clay modification and compatibilizers on the formation and physical properties of melt-mixed polypropylene/clay nanocomposites " *Polymer Science,* **42**(2004), 4139-4150.

15 F.G. Ramos, T.A. Melo, M.S. Rabello, and S.M. Silva. "Thermal stability of nanocomposites based on polypropylene and bentonite" *Polymer Degradation and Stability*, **89**(2005), 383-392.

16 N. Othman, H. Ismail and M. Mariatti "Effect of compatibilizers on mechanical and thermal properties of bentonite filled polypropylene composites" *Polymer Degradation and Stability*, **91**(2006), 1761-1774.

17 L. Szazdi, B. Pkanszky Jr, G.J. Vancso, and B. Pukanszky. "Quantitative estimation of the reinforcing effect of layered silicates in PP nanocomposites" *Polymer,* **47**(2006), 4638-4648.

18 N. Fedullo, E. Sorlier, M. Sclavons, C. Bailly, J. Lefebvre, and J. Devaux. "Polymer-based nanocomposites: Overview, application and perspectives" *Progress in Organic Coatings,* **58**(2007), 87-95.

19 M. Frounchi, S. Dadbin, Z. Salehpour, and M. Noferesi. "Gas barrier properties of PP/EPDM blend nanocomposites" *Journal of Membrane Science,* **282**(2006), 146-148.

20 H. Krump, A.S. Luyt, and I. Hudec. "Effect of different modified clays on the thermal and physical properties of polypropylene-montmorillonite nanocomposites" *Materials Letters,* **60**(2006), 2877-2880.